




TECHNICAL ARTICLE

Recovery of Copper, Lead, Zinc, and Arsenic from Copper Smelting Dust by Oxidative Alkaline Leaching and Sulfide Precipitation

LEI TIAN ^{1,3,4}, JIACONG XU^{1,3}, QIN YI^{1,3}, AO GONG^{1,3},
SHENGHUI WEN^{1,3}, RUIXIANG WANG^{1,3} and ZHIFENG XU^{1,2,3}

1.—Jiangxi Univ Sci and Technol, Inst Green Met and Proc Intensificat, Ganzhou 341000, People's Republic of China. 2.—Jiangxi College of Applied Technology, Ganzhou 341000, People's Republic of China. 3.—Key Laboratory of Ionic Rare Earth Resources and Environment, Ministry of Natural Resources, Ganzhou 341000, Jiangxi, People's Republic of China. 4.—e-mail: tianleijx@163.com

The separation of Cu, Pb, Zn, and As from copper smelting dust through oxidative alkali leaching and sulfide precipitation, as well as the subsequent recovery of As through calcification precipitation and carbothermal reduction, were realized in this study to utilize resources from and safely treat copper smelting dust. The binding behavior of As(V) to As(III) with S ions in the solution was analyzed through thermodynamic calculations. The separation rates of Cu, Pb, Zn, and As after oxidative alkali leaching and sulfide precipitation were 98.22%, 82%, 94.6%, and 99.27%, respectively, and the residual rate of S ions in the solution was only 3.6%. X-ray diffraction and scanning electron microscopy/energy-dispersive X-ray spectroscopy were employed to characterize the phase transformation and surface morphology of the metals during leaching. It was determined that Cu existed in the alkaline leaching residue in the form of $\text{Cu}(\text{OH})_2$, and that Pb and Zn existed in the sulfide residue as sulfides. As was deposited from the As solution in the simplest form as elemental As through calcification precipitation and the reduction of the As residue, and there was no residual CaS in the reduction residue, making it recyclable.

INTRODUCTION

Approximately 85% of the global Cu production is achieved through pyrometallurgical processes, which produce approximately 2.3 million tons of hazardous copper smelting dust annually.^{1–3} Copper smelting dust contains valuable metals, such as Cu, Zn, Bi, and In, as well as toxic metals, such as As, Pb, and Cd, which have significant recovery values.^{4–8} The yield of hazardous smelting dust is currently approximately 10% that of refined Cu.⁹

Lei Tian and Jiaciong Xu have contributed equally to this work and share senior authorship.

(Received December 6, 2022; accepted June 29, 2023; published online July 24, 2023)

As is the main hazardous element in smelting dust waste. Owing to its high toxicity, carcinogenicity, and diffusion rate, copper smelting dust poses a significant risk to the global ecosystem, human health, and sustainable development.^{10–14} The safe treatment and resource utilization of copper smelting dust are imperative considerations when recycling it. Therefore, the development of a process that can not only recover valuable metals but also safely treat toxic As is vital.

The phase composition of the dust produced during copper smelting is complex and fluctuates considerably.¹⁵ Nevertheless, valuable metals can be recovered from copper smelting dust and recycled. In general, the processes for the comprehensive utilization and treatment of copper smelting dust resources can be classified into pyrometallurgical and hydrometallurgical. Pyrometallurgical

treatments are mainly used to separate valuable elements in copper smelting dust by exploiting the different boiling points of its components and recover valuable metals by oxidation and reduction.^{16–18} However, because of the fire treatment, high energy consumption, incomplete collection of As-containing dust, and other shortcomings of pyrometallurgical treatments, most copper smelting dust is treated through hydrometallurgical methods. For example, H_2SO_4 ,^{19,20} HCl ,²¹ NaHS-NaOH ,²² $\text{Na}_2\text{S-NaOH}$,^{23,24} NaOH-S ,²⁵ and other chemicals have been used to leach Cu soot so that the valuable metals are transferred into solutions or slags for subsequent recovery. The precipitation method is mainly used to treat As through the formation of As-containing waste residues.^{25–27} However, the large volume of As-containing waste residues generated requires a large amount of land for accumulation, and carries the risk of As leakage and subsequent secondary pollution. In acidic systems, the formation and volatilization of highly toxic AsH_3 should always be prevented during As separation. In comparison, As concentration can be achieved more safely in alkaline systems. Guo et al.²³ used an $\text{NaOH-Na}_2\text{S}$ system to treat high-As dust. Under the conditions of an alkali/dust mass ratio of 0.5, sodium sulfide of 0.25 g/g, leaching temperature of 90°C, leaching time of 2 h, and liquid/solid (L/S) ratio of 5:1, the leaching rate of As could reach 92.75%, and the obtained residue constituted an available Pb resource. Zhang et al.²⁵ studied the removal of As from high-As copper smelting soot using a NaOH-S system, in which the leaching of Pd, Cu, Sb, and other elements in the soot was inhibited by introducing elemental S. The leaching rate of As reached 99.8% under optimal conditions. Despite the ability of these alkaline system treatments to separate As from valuable metals, Cu, Pb, Zn, and other valuable metals enter the slag and can only be used after subsequent treatment and separation; further, the consumption of Na_2S or S is higher. Some scholars usually use high-temperature, high-pressure assistance, or mechanical activation to enhance the utilization rate of leaching agents and enhance the leaching rate.^{23,28–30}

In this paper, a process is proposed for the resource recovery of Cu, Pb, Zn, and As in an alkaline system. In the first step, Cu is separated by oxidative alkali leaching; in the second step, Pb and Zn are recovered through sulfide precipitation; and, in the last step, As is treated safely by precipitation and reduction. This process can not only recover Cu, Pb, Zn, and other valuable metals in a stepwise manner but also consumes less Na_2S and recycles As. The optimum conditions were determined by evaluating the process performance. The relationship between the leaching behaviors of Cu, As, Pb, and Zn was studied, and X-ray diffraction (XRD) and scanning electron microscopy/energy-dispersive

X-ray spectroscopy (SEM/EDS) were used to characterize the phase transformation and surface morphology of the metals during leaching.

EXPERIMENTAL

Materials

Copper smelting dust samples were collected from the blast furnace smelting of copper dross in a copper smelter in Henan Province, China. The collected samples were dried, ground, and sieved using a 100-mesh sieve. Their XRD patterns and chemical compositions are shown in Fig. 1 and Table I, respectively. Cu, Pb, Zn, and As were detected using inductively coupled plasma (ICP) spectrometry. They constituted more than 40% of the samples, indicating the high recovery value for these valuable metals. The XRD results showed that the copper smelting dust was mainly composed of CuSO_4 , PbSO_4 , ZnSO_4 , As_2O_3 , and $\text{Fe}_2(\text{SO}_4)_3$.

Experimental

In the first step of this experiment, Cu was separated from Pb, Zn, and As by oxidative alkali leaching. Cu entered the alkali leaching residue in the form of copper hydroxide. In the second step, Pb and Zn were separated from As by sulfide precipitation and deposited in the slag in the form of sulfides. Finally, the As-containing solution was treated with calcium oxide for As removal, and the resulting As residue was reduced to obtain elemental As, which can be used as a resource. The flowchart of the process is shown in Fig. 2.

The oxidative alkali leaching, sulfide precipitation, and As deposition experiments were performed in an atmospheric-pressure stirring leaching device, and the fire reduction experiments were performed in a tube furnace. Before each experiment, a sodium hydroxide (NaOH) solution was prepared in the desired concentration and volume and placed in a beaker. Then 20 g of Cu soot were mixed with the

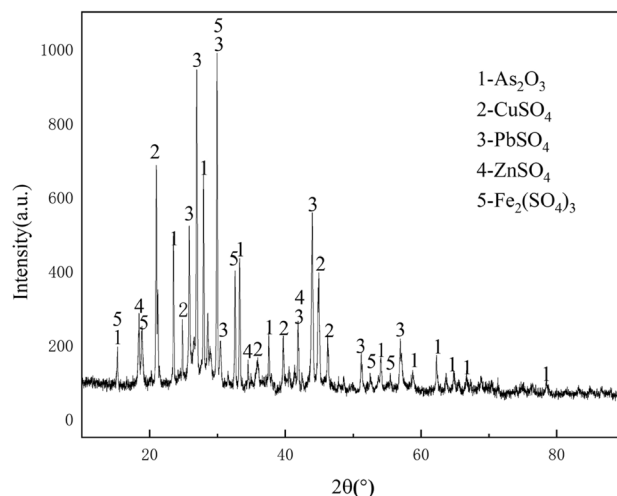


Fig. 1. XRD pattern of copper smelting dust.

NaOH solution and heated in a water bath at a constant temperature and set stirring speed. During leaching, hydrogen peroxide was slowly dropped into the solution, and 200 mL of the alkali leaching solution was used for the sulfide precipitation experiment. The required amount of $\text{Na}_2\text{S}\cdot 9\text{H}_2\text{O}$ was added to the alkali leaching solution, following which the stirring speed and required temperature were set for the subsequent experiments. For the As sedimentation experiment, 200 mL of the vulcanized liquid was used, and the required amount of CaO was added. The stirring rate and reaction temperature were set for the subsequent experiments. A total of 5 g of As sediment and the required amount of toner were thoroughly mixed, added to a crucible, and placed in a tube furnace for reaction. At the end of each experiment, the residue from the reaction was dried, weighed, and ground, and its chemical composition was analyzed. The leached liquid was measured by a measuring cylinder and analyzed using ICP spectrometry.

Evaluation Factors and Characterization

The main evaluation factors for the leaching behavior of Cu, Pb, Zn, and As in Cu soot are the

Table I. Main chemical components of copper smelting dust (wt.%)

As	Pb	Zn	Cu	Fe	S	O	Other
10.74	19.92	2.64	9.6	0.48	11.32	40.16	5.14

leaching and precipitation rates, as expressed in Eqs. 1 and 2, respectively. The leaching and precipitation rates of the elements during the oxidative alkali leaching and sulfide precipitation processes were calculated as:

(1) Element leaching rate

$$\varphi = \frac{C \times V}{m \times \omega} \times 100\% \tag{1}$$

where φ is the leaching rate of Cu, Pb, Zn or As, C is the metal concentration in g/L, V is the volume of the leaching solution in L, m is the quantity of the materials in g, and ω is the metal content in the materials in %.

(2) Element precipitation rate

$$\varepsilon = \frac{C_1 \times V_0 - C_2 \times V_t}{C_1 \times V_0} \times 100\% \tag{2}$$

where ε is the precipitation rate of Pb or Zn, C_1 and C_2 are the element concentrations before and after sulfide precipitation in g/L, respectively, and V_0 and V_t are the volumes of the solution before and after sulfide precipitation in L, respectively.

The chemical compositions of the samples were determined using ICP spectrometry. XRD and SEM/EDS were employed to characterize the phase composition and surface morphology of the raw materials and leached residues, respectively.

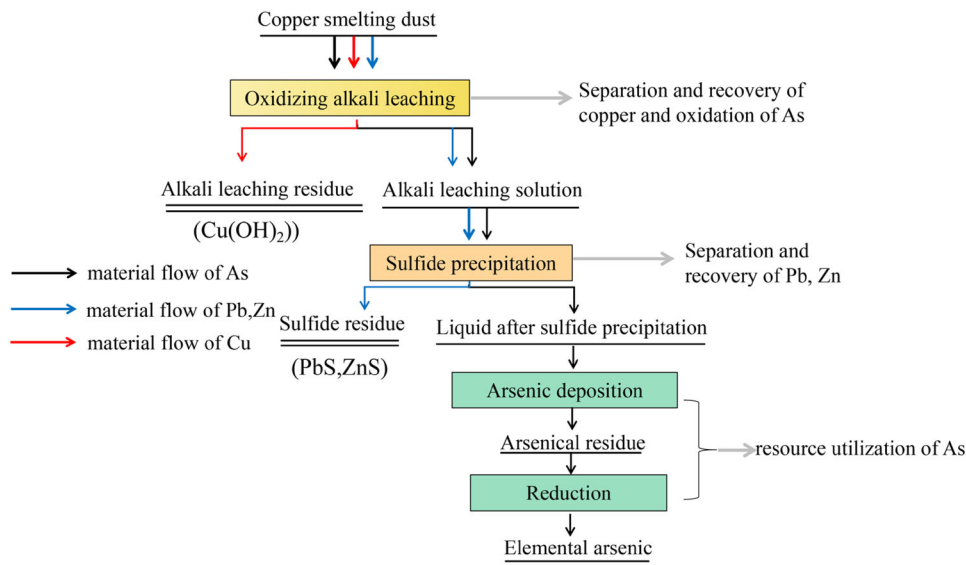
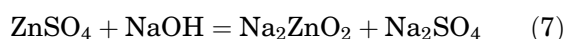
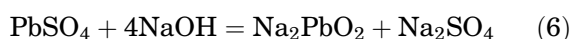
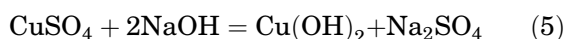
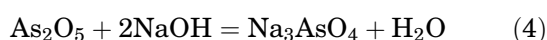


Fig. 2. Process flow chart.

RESULTS AND DISCUSSION

Separation of Cu by Oxidative Alkaline Leaching

As exists in the form of arsenic trioxide in Cu soot and mainly in the form of arsenite in the alkaline system, although oxidized arsenite has a higher solubility in the latter.^{31,32} As can exist under alkaline conditions, Pb and Zn need to have a pH greater than 12 to exist under alkaline conditions, while Cu cannot exist under this condition.^{33,34} The differences between the leaching behaviors of Cu, Pb, Zn, and As under alkaline conditions were exploited to separate these elements through the following chemical reactions:



Effect of Leaching Temperature

The effect of the leaching temperature from 30°C to 90°C was studied at a NaOH concentration of 3.0 mol/L, leaching time of 60 min, L/S ratio of 6:1, H₂O₂ addition of 1.2 times the molar ratio of H₂O₂/As₂O₃, and agitation speed of 300 rpm. The results are shown in Fig. 3a. As, Pb, and Zn leached slowly as the temperature increased from 30°C to 60°C. As the temperature exceeded 60°C and increased to 90°C, the leaching rates of As, Pb, and Zn increased. The main reasons for this increase are the decrease in the slurry viscosity and the increase in the diffusion of the reactant species as the leaching temperature increased. However, the leaching rate of Cu stabilized at a low level with increasing temperature. The optimal leaching temperature was therefore determined as 90°C.

Effect of Leaching Time

The effect of the leaching time from 20 min to 60 min was studied under a NaOH concentration of 3.0 mol/L, leaching temperature of 90°C, L/S ratio of 6:1, H₂O₂ addition of 1.2 times the molar ratio of H₂O₂/As₂O₃, and agitation speed of 300 rpm. The results presented in Fig. 3b show that the leaching rates of As, Pb, and Zn increased with the leaching time, especially from 20 min to 60 min. Beyond 60 min, the leaching rates of As, Pb, and Zn changed slightly as the leaching temperature increased. However, the Cu leaching rate remained

low. The optimum leaching time was therefore determined as 90 min.

Effect of Liquid/Solid Ratio

The effect of the L/S ratio from 4:1 to 8:1 min was studied under a NaOH concentration of 3.0 mol/L, leaching temperature of 90°C, leaching time of 60 min, H₂O₂ addition of 1.2 times the molar ratio of H₂O₂/As₂O₃, and agitation speed of 300 rpm. The results are shown in Fig. 3c. As the L/S ratio increased from 4:1 to 8:1, the leaching rates of As, Pb, and Zn gradually increased. The leaching rates did not change significantly with further increases in the L/S ratio. The As, Pb, and Zn leaching rates increased with the L/S ratio because, as the ratio increased, the fluidity of the solution increased, which increased the contact area between the solid and liquid phases and caused more reactants to come into contact with the leaching solution. The Cu leaching rate was stable at a low level, as before. The optimal L/S ratio was thus determined to be 8:1.

Effect of NaOH Concentration

The NaOH concentration plays an important role in the separation of As. The effect of the NaOH concentration from 1.5 mol/L to 3.0 mol/L min was studied under a L/S ratio of 6:1, leaching temperature of 90°C, leaching time of 60 min, H₂O₂ addition of 1.2 times the molar ratio of H₂O₂/As₂O₃, and agitation speed of 300 rpm. The results are shown in Fig. 3d. Increasing the NaOH concentration from 1.5 mol/L to 3 mol/L had a particularly notable effect on increasing the leaching rates of As, Pb, and Zn. The leaching rate of As reached its highest value at the concentration of 3.5 mol/L. Further increases in the alkali concentration had little effect on the leaching rate of As. Although the leaching rates of Pb and Zn increased with increasing alkali concentration, the increases were small and the leaching rate of Cu remained low. Significantly increasing the NaOH concentration can further improve the leaching rate, but at this point, the leaching rate of copper will increase significantly. The optimal alkali concentration was therefore 3.5 mol/L.

Based on the above experiments, the optimum conditions were determined as a NaOH concentration of 3.0 mol/L, leaching temperature of 90°C, leaching time of 60 min, L/S ratio of 8:1, H₂O₂ addition of 1.2 times the molar ratio of H₂O₂/As₂O₃, and agitation speed of 300 rpm. Under these conditions, the leaching rates of As, Pb, Zn, and Cu were 99.27%, 82.82%, 95.60%, and 1.78%, respectively. The XRD pattern of the alkali leaching residue is shown in Fig. 4a. The results show that Cu exists in the alkaline leaching residue in the form of Cu(OH)₂ with poor grain crystallinity. The SEM/EDS results for the alkali leaching residue are shown in Fig. 4b. The SEM image shows that the particles in the alkali leaching residue are irregularly distributed

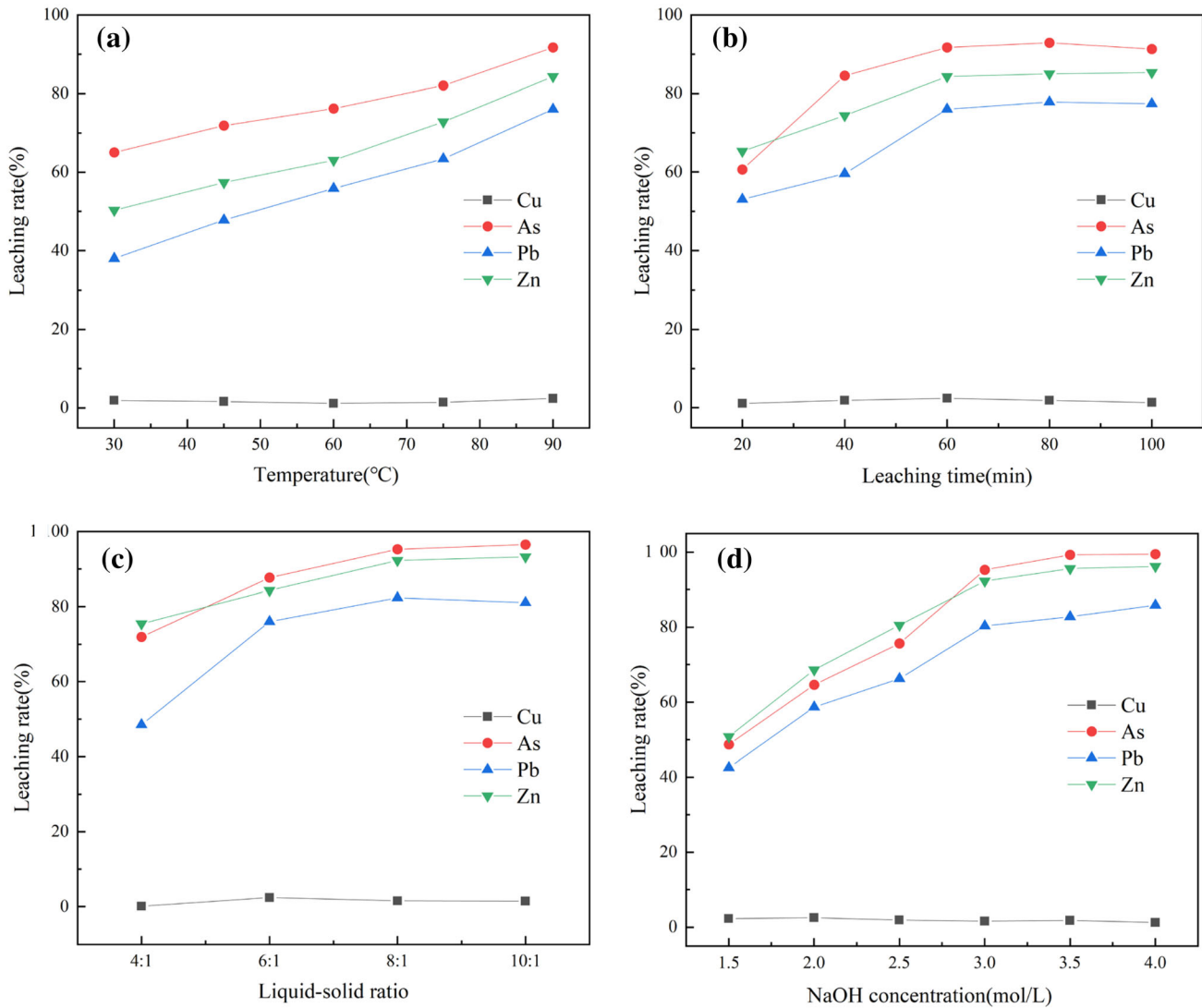


Fig. 3. (a) Effect of leaching temperature on leaching rates of As, Pb, Zn, and Cu, (b) effect of leaching time on leaching rates of As, Pb, Zn, and Cu, (c) effect of liquid/solid ratio on leaching rates of As, Pb, Zn, and Cu, and (d) effect of NaOH concentration on leaching rates of As, Pb, Zn, and Cu.

and uneven in shape, and it can be seen from points 1 and 2 in the EDS profile that the alkali leaching residue is mainly composed of Cu, H, and O, with a high Cu content.

Separation of Pb Zn by Sulfide Precipitation

Thermodynamic Analysis

As exists in alkaline systems in the form of arsenite or arsenate, both of which combine with added S ions to form thioarsenite and thioarsenate. However, when excess S ions are subsequently used to precipitate As with calcium oxide, calcium sulfide is precipitated.³⁵ The resultant precipitate cannot be removed during the subsequent fire reduction, which inhibits the recycling of the reduction slag (calcium oxide). Therefore, to mitigate the combination of excess S ions with As in the solution, it is necessary to determine the ability of As (III) and As

(V) to combine with S ions under alkaline conditions. The optimal form of As in solution was therefore determined.

The equilibrium relationship (298 K) between As(III)-S-H₂O and As(V)-S-H₂O is presented in Tables II and III. By calculating the concentrations of thioarsenate and thioarsenious acid in systems with different S/As ratios under alkaline conditions, the binding ability of As(III) and As(V) to S ions under alkaline conditions can be determined. Because of the complexity of thioarsenate, its binding ability was calculated from [S] ([S] = [HS⁻] + [S²⁻] + [H₂S]) in solution. In alkaline systems, As(III) may exist as H_xAsO₃^{x-3}, H_xAsO₂S^{x-3}, H_xAsOS₂^{x-3}, and H_xAsS₃^{x-3} (x = 1, 2, 3). Therefore, based on the substance conservation rule, the relationships between the concentrations of As in various forms in the As(III)-S-H₂O system can be obtained as

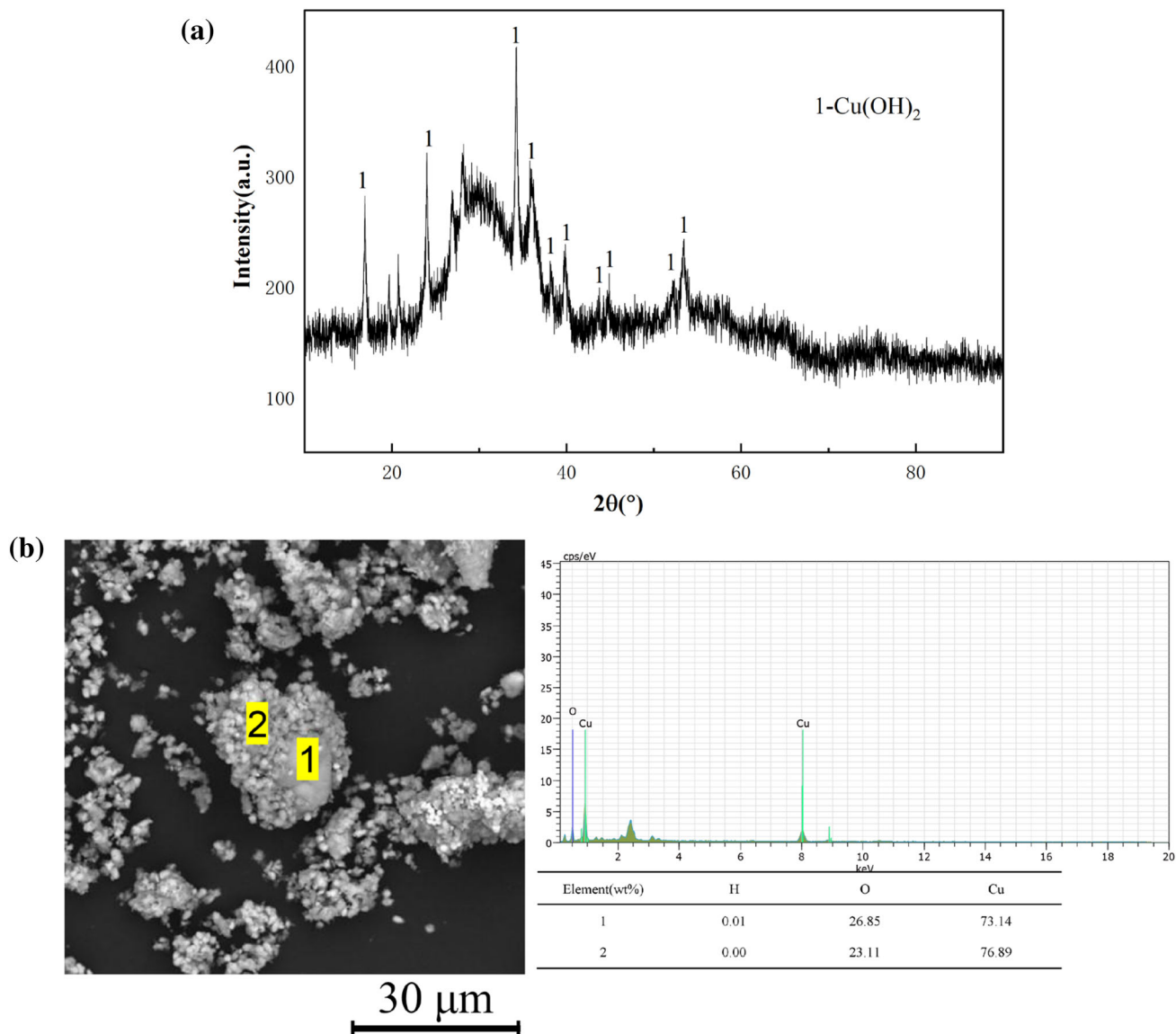
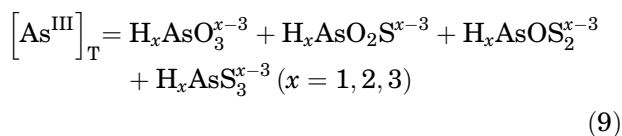
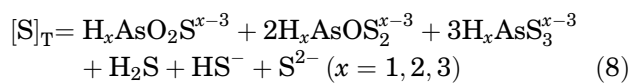
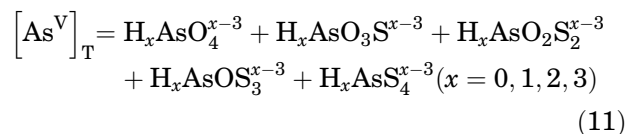
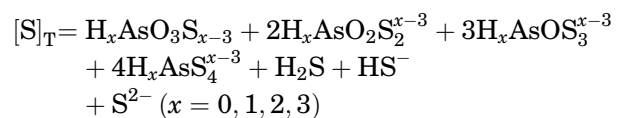


Fig. 4. (a) XRD pattern of alkali leaching residue, (b) SEM/EDS results for alkali leaching residue.



Similarly, the relationships between the concentrations of As in various forms in the As(V)-S-H₂O system can be obtained as:



The concentrations of the ions at each given pH level and S/As ratio (molar ratios) can be solved simultaneously, based on the concentration relationships mentioned above. Because the S/As ratios

Table II. Equilibrium relationships in the As(V)-S-H₂O system

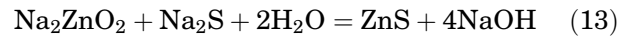
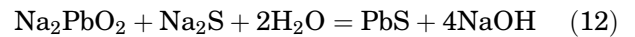
	Equilibrium relationship	Concentration relationship
1	$\text{H}_3\text{AsO}_4 + \text{H}_2\text{S}(\text{aq}) = \text{H}_3\text{AsSO}_3 + \text{H}_2\text{O}$	$[\text{H}_3\text{AsSO}_3] = 10^{0.4}[\text{H}_3\text{AsO}_4][\text{H}_2\text{S}]$
2	$\text{H}_3\text{AsSO}_3 + \text{H}_2\text{S}(\text{aq}) = \text{H}_3\text{AsS}_2\text{O}_2 + \text{H}_2\text{O}$	$[\text{H}_3\text{AsS}_2\text{O}_2] = 10^{0.1}[\text{H}_3\text{AsSO}_3][\text{H}_2\text{S}]$
3	$\text{H}_3\text{AsS}_2\text{O}_2 + \text{H}_2\text{S}(\text{aq}) = \text{H}_3\text{AsS}_3\text{O} + \text{H}_2\text{O}$	$[\text{H}_3\text{AsS}_3\text{O}] = 10^{3.5}[\text{H}_3\text{AsS}_2\text{O}_2][\text{H}_2\text{S}]$
4	$\text{H}_3\text{AsS}_3\text{O} + \text{H}_2\text{S}(\text{aq}) = \text{H}_3\text{AsS}_4 + \text{H}_2\text{O}$	$[\text{H}_3\text{AsS}_4] = 10^{2.6}[\text{H}_3\text{AsS}_3\text{O}][\text{H}_2\text{S}]$
5	$\text{H}_2\text{S}(\text{aq}) = \text{HS}^- + \text{H}^+$	$[\text{HS}^-][\text{H}^+] = 10^{-7}[\text{H}_2\text{S}]$
6	$\text{HS}^- = \text{S}^{2-} + \text{H}^+$	$[\text{S}^{2-}][\text{H}^+] = 10^{-17}[\text{HS}^-]$
7	$\text{H}_3\text{AsO}_4 = \text{H}_2\text{AsO}_4^- + \text{H}^+$	$[\text{H}_2\text{AsO}_4^-][\text{H}^+] = 10^{-2.3}[\text{H}_3\text{AsO}_4]$
8	$\text{H}_2\text{AsO}_4^- = \text{HAsO}_4^{2-} + \text{H}^+$	$[\text{HAsO}_4^{2-}][\text{H}^+] = 10^{-7}[\text{H}_2\text{AsO}_4^-]$
9	$\text{HAsO}_4^{2-} = \text{AsO}_4^{3-} + \text{H}^+$	$[\text{AsO}_4^{3-}][\text{H}^+] = 10^{-11.8}[\text{HAsO}_4^{2-}]$
10	$\text{H}_3\text{AsSO}_3 = \text{H}_2\text{AsSO}_3^- + \text{H}^+$	$[\text{H}_2\text{AsSO}_3^-][\text{H}^+] = 10^{-3.3}[\text{H}_3\text{AsSO}_3]$
11	$\text{H}_2\text{AsSO}_3^- = \text{HASO}_3^{2-} + \text{H}^+$	$[\text{HASO}_3^{2-}][\text{H}^+] = 10^{-7.2}[\text{H}_2\text{AsSO}_3^-]$
12	$\text{HASO}_3^{2-} = \text{AsSO}_3^{3-} + \text{H}^+$	$[\text{AsSO}_3^{3-}][\text{H}^+] = 10^{-11}[\text{HASO}_3^{2-}]$
13	$\text{H}_3\text{AsS}_2\text{O}_2 = \text{H}_2\text{AsS}_2\text{O}_2^- + \text{H}^+$	$[\text{H}_2\text{AsS}_2\text{O}_2^-][\text{H}^+] = 10^{2.4}[\text{H}_3\text{AsS}_2\text{O}_2]$
14	$\text{H}_2\text{AsS}_2\text{O}_2^- = \text{HAS}_2\text{O}_2^{2-} + \text{H}^+$	$[\text{HAS}_2\text{O}_2^{2-}][\text{H}^+] = 10^{-7.1}[\text{H}_2\text{AsS}_2\text{O}_2^-]$
15	$\text{HAS}_2\text{O}_2^{2-} = \text{AsS}_2\text{O}_2^{3-} + \text{H}^+$	$[\text{AsS}_2\text{O}_2^{3-}][\text{H}^+] = 10^{-10.8}[\text{HAS}_2\text{O}_2^{2-}]$
16	$\text{H}_3\text{AsS}_3\text{O} = \text{H}_2\text{AsS}_3\text{O}^- + \text{H}^+$	$[\text{H}_2\text{AsS}_3\text{O}^-][\text{H}^+] = 10^{1.7}[\text{H}_3\text{AsS}_3\text{O}]$
17	$\text{H}_2\text{AsS}_3\text{O}^- = \text{HAS}_3\text{O}_2^- + \text{H}^+$	$[\text{HAS}_3\text{O}_2^-][\text{H}^+] = 10^{-1.5}[\text{H}_2\text{AsS}_3\text{O}^-]$
18	$\text{HAS}_3\text{O}_2^- = \text{AsS}_3\text{O}^{3-} + \text{H}^+$	$[\text{AsS}_3\text{O}^{3-}][\text{H}^+] = 10^{-10.8}[\text{HAS}_3\text{O}_2^-]$
19	$\text{H}_3\text{AsS}_4 = \text{H}_2\text{AsS}_4^- + \text{H}^+$	$[\text{H}_2\text{AsS}_4^-][\text{H}^+] = 10^{2.3}[\text{H}_3\text{AsS}_4]$
20	$\text{H}_2\text{AsS}_4^- = \text{HAS}_4^{2-} + \text{H}^+$	$[\text{HAS}_4^{2-}][\text{H}^+] = 10^{-1.5}[\text{H}_2\text{AsS}_4^-]$
21	$\text{HAS}_4^{2-} = \text{AsS}_4^{3-} + \text{H}^+$	$[\text{AsS}_4^{3-}][\text{H}^+] = 10^{-5.2}[\text{HAS}_4^{2-}]$

Table III. Equilibrium relationships in the As(III)-S-H₂O system

	Equilibrium relationship	Concentration relationship
1	$\text{H}_3\text{AsO}_3 + \text{H}_2\text{S}(\text{aq}) = \text{H}_3\text{AsSO}_2 + \text{H}_2\text{O}$	$[\text{H}_3\text{AsSO}_2] = 10^{11}[\text{H}_3\text{AsO}_3][\text{H}_2\text{S}]$
2	$\text{H}_3\text{AsSO}_2 + \text{H}_2\text{S}(\text{aq}) = \text{H}_3\text{AsS}_2\text{O} + \text{H}_2\text{O}$	$[\text{H}_3\text{AsS}_2\text{O}] = 10^{3.8}[\text{H}_3\text{AsSO}_2][\text{H}_2\text{S}]$
3	$\text{H}_3\text{AsS}_2\text{O} + \text{H}_2\text{S}(\text{aq}) = \text{H}_3\text{AsS}_3 + \text{H}_2\text{O}$	$[\text{H}_3\text{AsS}_3] = 10^{5.6}[\text{H}_3\text{AsS}_2\text{O}][\text{H}_2\text{S}]$
4	$\text{H}_2\text{S}(\text{aq}) = \text{HS}^- + \text{H}^+$	$[\text{HS}^-][\text{H}^+] = 10^{-7}[\text{H}_2\text{S}]$
5	$\text{HS}^- = \text{S}^{2-} + \text{H}^+$	$[\text{S}^{2-}][\text{H}^+] = 10^{-17}[\text{HS}^-]$
6	$\text{H}_3\text{AsO}_3 = \text{H}_2\text{AsO}_3^- + \text{H}^+$	$[\text{H}_2\text{AsO}_3^-][\text{H}^+] = 10^{-9.17}[\text{H}_3\text{AsO}_3]$
7	$\text{H}_2\text{AsO}_3^- = \text{HASO}_3^- + \text{H}^+$	$[\text{HASO}_3^-][\text{H}^+] = 10^{-14.1}[\text{H}_2\text{AsO}_3^-]$
8	$\text{H}_3\text{AsSO}_2 = \text{H}_2\text{AsSO}_2^- + \text{H}^+$	$[\text{H}_2\text{AsSO}_2^-][\text{H}^+] = 10^{-3.7}[\text{H}_3\text{AsSO}_2]$
9	$\text{H}_2\text{AsSO}_2^- = \text{HASO}_2^{2-} + \text{H}^+$	$[\text{HASO}_2^{2-}][\text{H}^+] = 10^{-14.1}[\text{H}_2\text{AsSO}_2^-]$
10	$\text{H}_3\text{AsS}_2\text{O} = \text{H}_2\text{AsS}_2\text{O}^- + \text{H}^+$	$[\text{H}_2\text{AsS}_2\text{O}^-][\text{H}^+] = 10^{-3.7}[\text{H}_3\text{AsS}_2\text{O}]$
11	$\text{H}_2\text{AsS}_2\text{O}^- = \text{HAS}_2\text{O}^{2-} + \text{H}^+$	$[\text{HAS}_2\text{O}^{2-}][\text{H}^+] = 10^{-8.6}[\text{H}_2\text{AsS}_2\text{O}^-]$
12	$\text{H}_3\text{AsS}_3 = \text{H}_2\text{AsS}_3^- + \text{H}^+$	$[\text{H}_2\text{AsS}_3^-][\text{H}^+] = 10^{-3.7}[\text{H}_3\text{AsS}_3]$
13	$\text{H}_2\text{AsS}_3^- = \text{HAS}_3^{2-} + \text{H}^+$	$[\text{HAS}_3^{2-}][\text{H}^+] = 10^{-8.6}[\text{H}_2\text{AsS}_3^-]$

were generally low during the vulcanization experiment, only S/As ratios lower than or equal to 4 were considered. The relationships between $[\text{S}]/[\text{S}]_T$ in the As(V)-S-H₂O and As(III)-S-H₂O systems under different pH conditions are shown in Fig. 5, from which it can be seen that, under the same conditions, the proportion of [S] in the As(III) system is smaller than that in the As(V) system. This implies that the binding capacity of As(III) to S²⁻ is stronger than that of As(V). Therefore, the use of hydrogen peroxide to oxidize As(III) to As(V) in the alkaline leaching process cannot only increase the leaching rate of As in the alkaline system but also mitigate the subsequent combination of excess S ions with the As in the solution.

Alkali leaching solutions were used as the raw material and Na₂S as the precipitant in the sulfide precipitation experiment for separating Pb and Zn. The influence of three factors, namely, the amount of Na₂S added, reaction temperature, and reaction time, was investigated. The relevant chemical equations are:



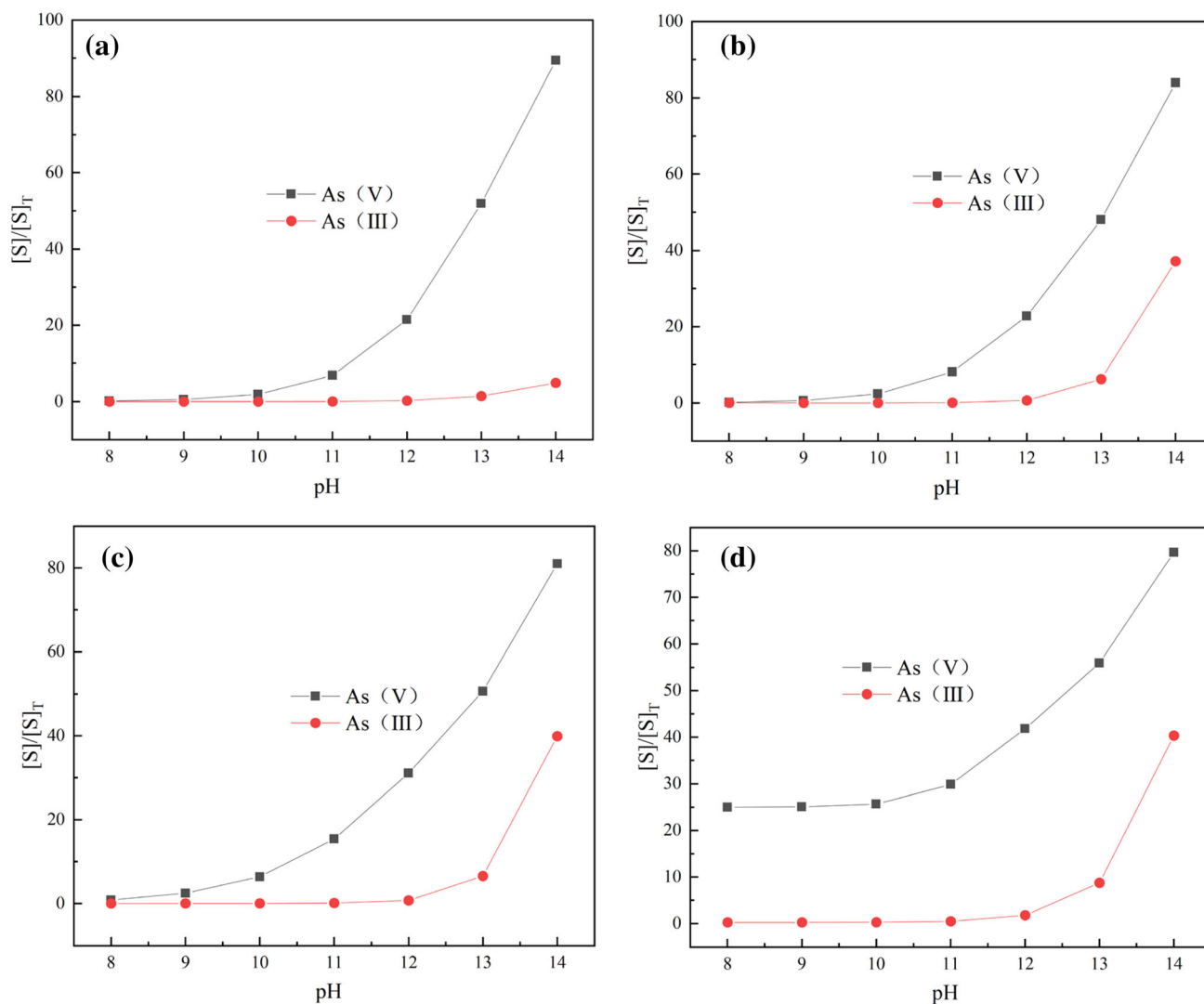


Fig. 5. (a) S/As = 1, (b) S/As = 2, (c) S/As = 3, and (d) S/As = 4.

Effect of Na_2S Addition

The effect of Na_2S addition was studied at a temperature of 80°C for a precipitation time of 60 min and agitation speed of 300 rpm. The results in Fig. 6a indicate that the precipitation rates of Pb and Zn change notably with the addition of Na_2S . The precipitation rates of Pb and Zn increased from 73.92% to 99.78% and from 2.20% to 99.5%, respectively, as the amount of Na_2S added increased from 0.8 to 1.2 times the theoretical quantity. Because the activity of lead sulfide is lower than that of zinc sulfide, Pb precipitates preferentially from the alkali leachate over Zn. All the Pb and Zn ions in the alkali leachate can be precipitated completely if Na_2S is fed continuously, although more S ions will be required. When the amount of added Na_2S is 1.2

times the theoretical quantity, the precipitation rates of Pb and Zn exceeded 99%, and the residual S ion concentration in the solution was only 3.6%. Therefore, the appropriate amount of Na_2S is approximately 1.2 times the theoretical quantity.

Effect of Precipitation Time

Figure 6b shows the effect of the precipitation time on the sulfide precipitation of Pb and Zn and the residual S ions in the solution with the addition of 1.2 times the theoretical quantity of Na_2S at a temperature of 80°C and an agitation speed of 300 rpm. The precipitation rates of Pb and Zn gradually increased with the precipitation time. At the precipitation time of 60 min, the precipitation rate exceeded 99% and a good precipitation effect

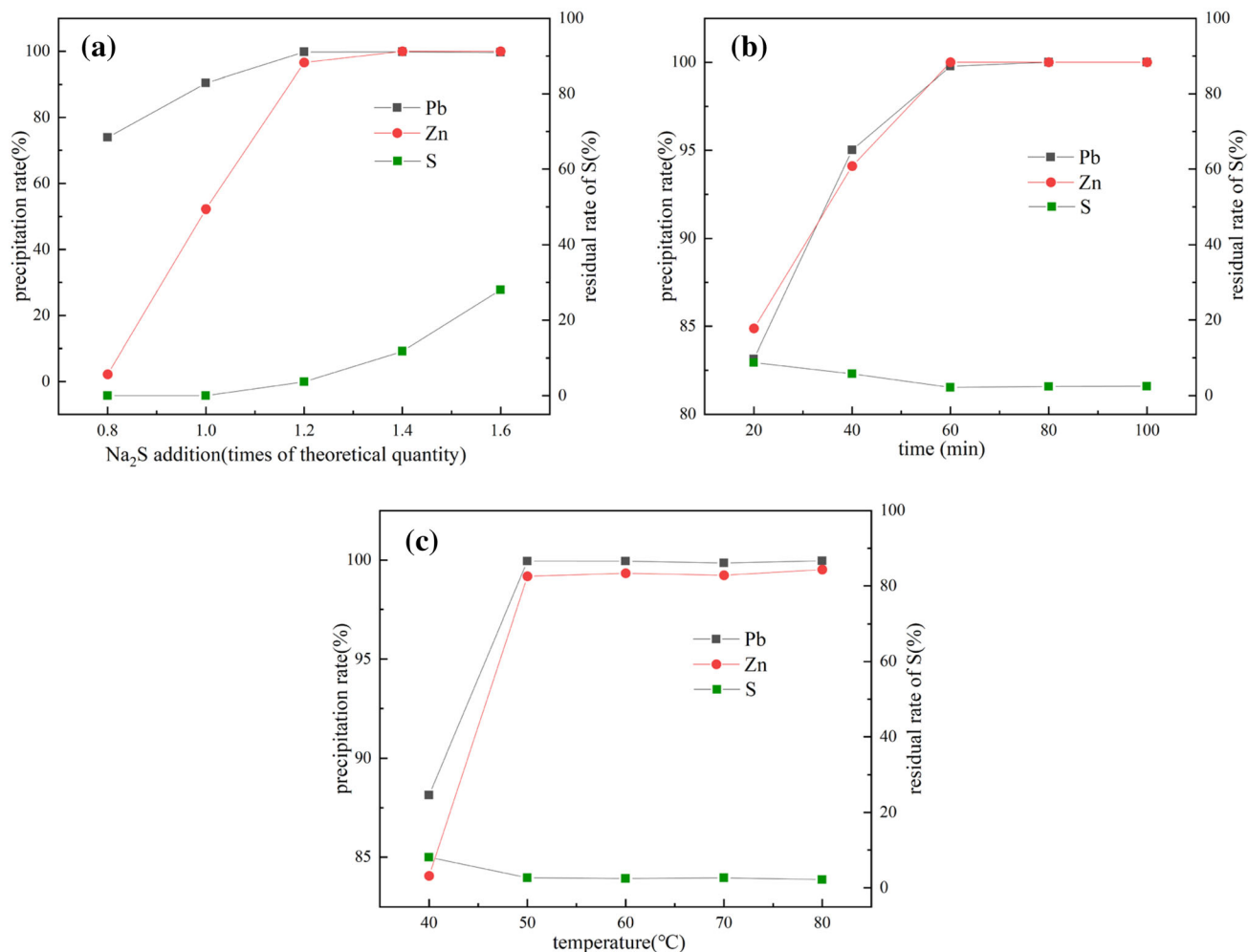


Fig. 6. (a) Effect of Na_2S addition on sulfide precipitation, (b) effect of precipitation time on sulfide precipitation, (c) effect of temperature on sulfide precipitation.

was achieved. The residual S ion content in the solution also decreased as the reaction proceeded. The optimum precipitation time was therefore determined to be 60 min.

Effect of Temperature

The effect of temperature was studied under the addition of 1.2 times the theoretical quantity of Na_2S , a precipitation time of 60 min, and agitation speed of 300 rpm. The results are shown in Fig. 6c. The precipitation rates of Pb and Zn increased from 88.14% to 99.78% and from 84.06% to 99.5%, respectively, as the temperature increased from 40 C to 50 C. At 50 $^{\circ}\text{C}$, Pb and Zn were separated and there were no notable changes when the temperature was increased further. As the temperature increased, the sulfide precipitation reaction occurred completely and the content of residual S ions in the solution was gradually reduced. Therefore, the temperature was set to 50 $^{\circ}\text{C}$.

Based on the experimental results, the optimum conditions were determined to be a temperature of 50 $^{\circ}\text{C}$, precipitation time of 60 min, agitation speed of 300 rpm, and the addition of 1.2 times the theoretical quantity of Na_2S . Compared with a system in which NaOH and Na_2S are added simultaneously, less Na_2S was used. Under these conditions, the precipitation rates of Pb and Zn exceeded 99%, and the residual rate of S ions was only 3.6%. The XRD and SEM/EDS results for the vulcanized slag are shown in Fig. 7a and b, respectively. The XRD results show that the main phases of the sulfide slag are PbS and ZnS. As can be seen from the SEM image, the sulfide slag has an inhomogeneous morphology and uneven distribution, and most of the slag particles are needle- or oval-shaped. The EDS profile shows that the elemental contents at three different points are mainly Pb, Zn, and S. The Pb content is the highest in the sulfide slag while the Zn content is lower, indicating that the

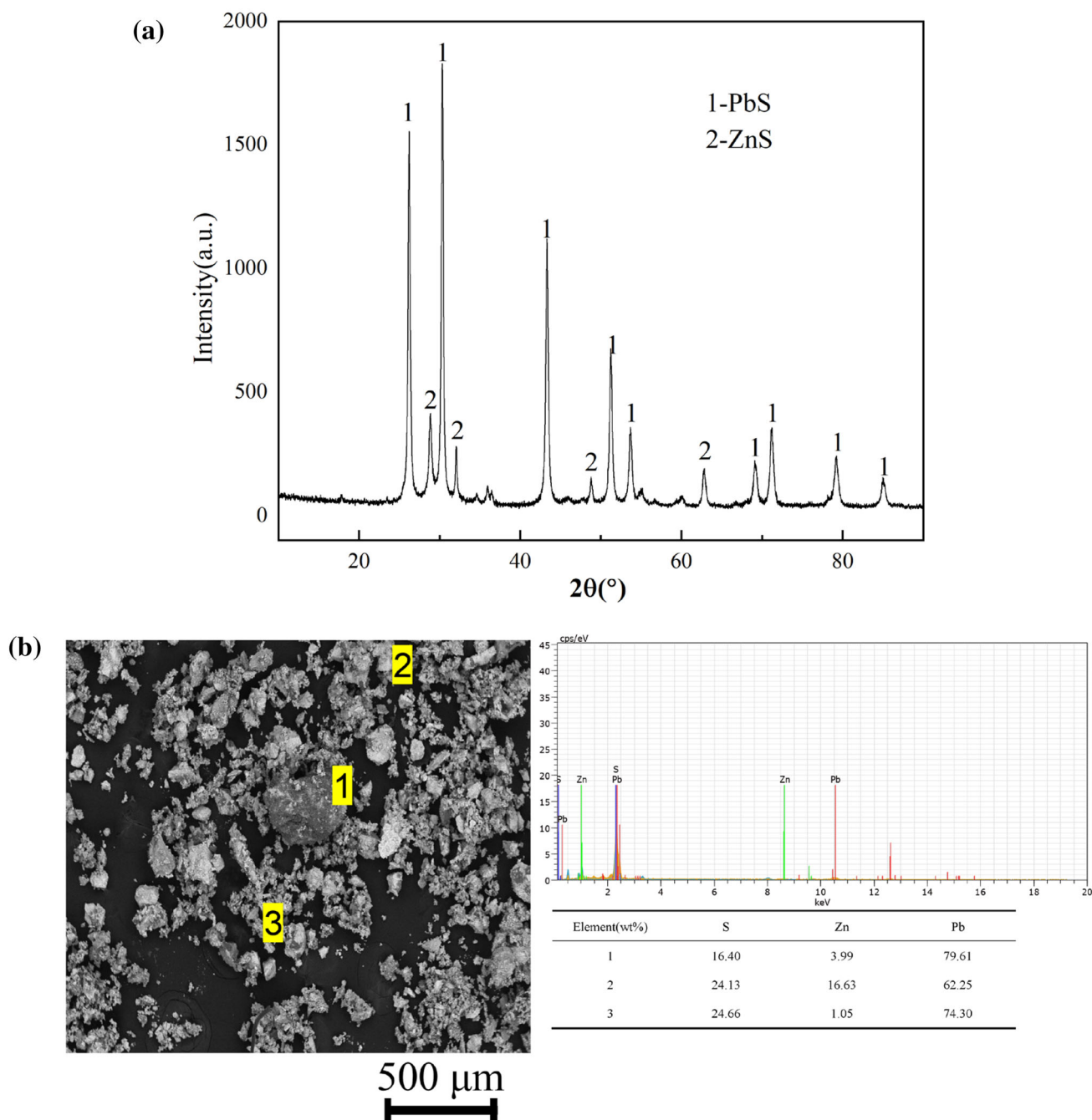


Fig. 7. (a) XRD pattern of sulfide residue, (b) SEM/EDS results for sulfide residue.

sulfide slag is primarily composed of Pb and S compounds and contains small amounts of Zn–S compounds.

Resource Utilization of As

The As solution obtained after sulfide precipitation was converted to As via calcium oxide precipitation and carbonation reduction. Compared to the As solution obtained by treating copper smelting dust with NaOH–Na₂S (Method 1), the As solution obtained by the oxidative alkaline leaching and

sulfide precipitation method (Method 2) proposed in this study contained fewer S ions and required less Na₂S. The As precipitation experiments were performed under the same process conditions. Method 1 was additionally supplemented with hydrogen peroxide for oxidation under the experimental conditions of a reaction temperature of 80°C, reaction time of 90 min, Ca/As molar ratio of 9, and stirring rate of 300 rpm.³⁶ The XRD patterns of the obtained As-precipitated slags are shown in Fig. 8a.

Figure 8a shows that the slags from Methods 1 and 2 contain Ca₅(AsO₄)₃OH, Ca₅(AsO₄)₃OH·H₂O,

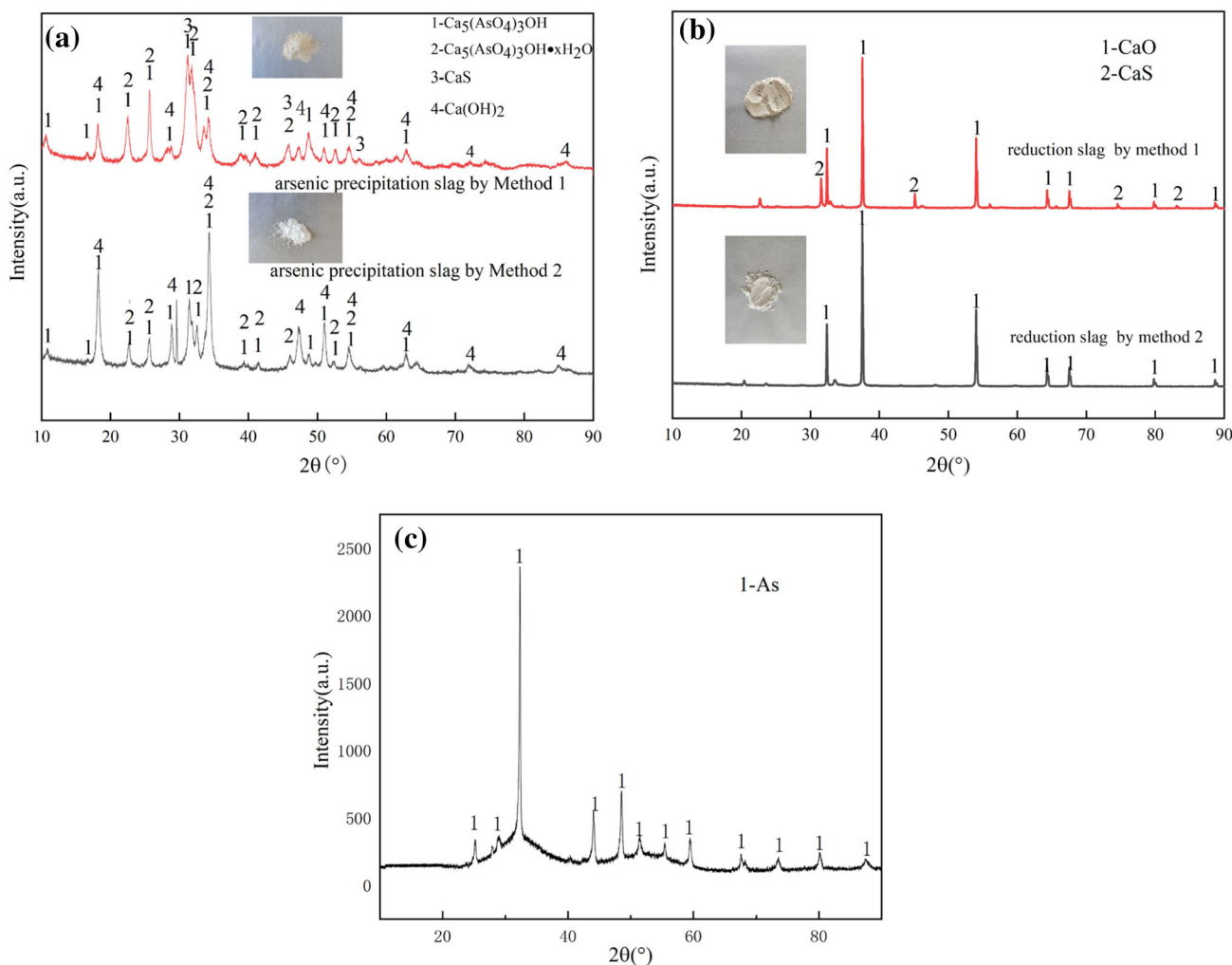


Fig. 8. (a) XRD patterns of As precipitation slags, (b) XRD patterns of reduction slags, (c) XRD pattern of volatile products.

and $\text{Ca}(\text{OH})_2$. The As precipitation slag obtained using Method 1 contains CaS, while that obtained using Method 2 does not. This indicates that calcium oxide reacts with the As solution that contains more S ions to produce CaS via calcium oxide precipitation.

Carbon thermal reduction was performed on the As precipitation slag obtained using Methods 1 and 2 with the process conditions of a reaction temperature of 1000°C , reaction time of 60 min, carbon allotment factor of 1.4, and Ar flow rate of $300\text{ mL}\cdot\text{min}^{-1}$. The XRD patterns of the reduction slag and collected volatile products are shown in Fig. 8b and c, respectively. Figure 8b shows that the physical phases of the reduction slag obtained using Method 1 are CaO and CaS, while that of the slag obtained using Method 2 is CaO, indicating that CaS remains in the reduction slag during the carbon reduction process and cannot be consumed. This reduces the efficiency of As precipitation, for which the reduction slag is subsequently. Toxic H_2S gas is

also produced when CaS reacts in the solution during recycling, which renders the process unsuitable for continuous use. The SEM images and EDS profiles of the reduction slags are shown in Fig. 9. The SEM images show that the agglomeration of the reduction slag obtained using Method 1 is more pronounced than that of the reduction slag obtained using Method 2. The EDS profiles at points 1 and 2 show that the S content in Method 1 is significantly higher than that in Method 2. This result indicates that excess S cannot be removed in the fire reduction of the slag obtained using Method 1. Quantitative analysis was conducted on the reduction slag of Method 1 using a carbon sulfur analyzer, and the results showed that the S content was only 0.95%, consistent with the comprehensive SEM/EDS results. The accumulation of this excess S in the reduction slag affects the suitability of the process for continuous use.

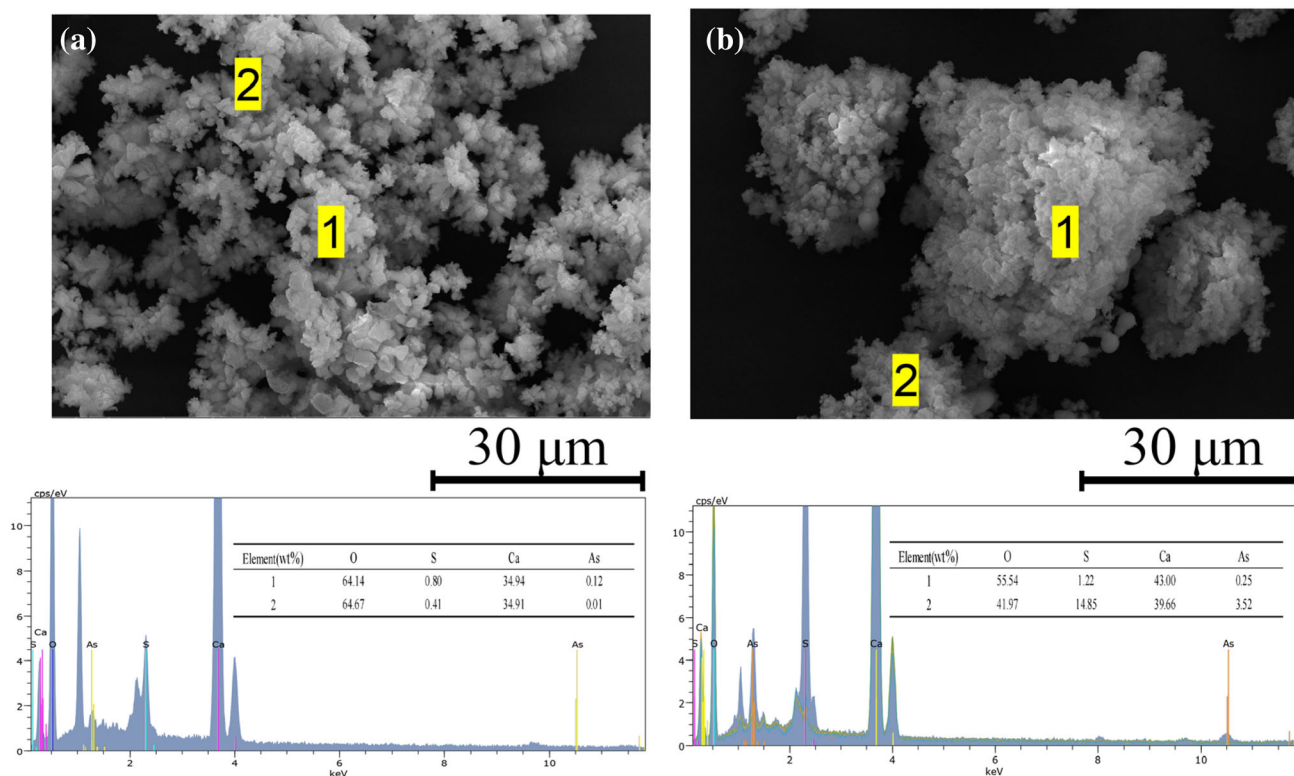


Fig. 9. SEM/EDS results for reduction slags: (a) Method 2, and (b) Method 1.

CONCLUSION

The separation of Cu from Pb, Zn, and As was realized by oxidative alkali leaching and sulfide precipitation, and As was subsequently recycled by calcification precipitation and carbothermal reduction. The following conclusions were drawn:

First, the effective separation of Cu, Pb, Zn, and As was achieved by oxidative alkaline leaching and sulfide precipitation. The leaching rates of As, Pb, Zn, and Cu under the optimal conditions for oxidative alkaline leaching were 99.27%, 82.82%, 95.60%, and 1.78%, respectively. Under the optimal conditions for sulfide precipitation, the precipitation rates of Pb and Zn exceeded 99%, the residual rate of S ions was only 3.6%, and the amount of Na_2S required was lower than that required in the simultaneous $\text{NaOH-Na}_2\text{S}$ system. The XRD and SEM/EDS characterization results showed that Cu entered the alkali leaching slag as $\text{Cu}(\text{OH})_2$, while Pb and Zn entered the sulfide slag as sulfides.

Second, through thermodynamic calculations, the magnitudes of $[\text{S}]/[\text{S}]_T$ in the As(V)-S- H_2O and As(III)-S- H_2O systems were obtained under the conditions of a S/As ratio lower than or equal to 4 and a pH range between 8 and 14. The results showed that As(V) had a weaker ability of combining with the S ions in the solution than As(III) and formed fewer thioarsenate ions.

Third, the XRD characterization results for the volatiles from the calcium precipitation of the As solution and the reduction of the precipitated As

slag indicated that the reduction product was elemental As. The recyclable reduction slag was free of CaS. Thus, the risk of H_2S generation during subsequent recycling was mitigated.

FUNDING

This work was supported and funded partly by the National Key R&D Program of China (No. 2019YFC1907405), the National Nature Science Foundation of China (Nos. 52064021 and 52074136), the Jiangxi Provincial Cultivation Program for Academic and Technical Leaders of Major Subjects (No. 20204BCJL23031), the Jiangxi Province Science Fund for Distinguished Young Scholars (No. 20202ACB213002), the Merit-based postdoctoral research in Jiangxi Province (No. 2019KY09), the Program of Qingjiang Excellent Young Talents, Jiangxi University of Science and Technology (No. JXUSTQJBJ2020004), Distinguished Professor Program of Jinggang Scholars in institutions of higher learning, Nature Science Foundation of Jiangxi Province (No. 2021ACB204015).

CONFLICT OF INTEREST

We declare that we have no financial and personal relationships with other people or organizations that can inappropriately influence our work, there is no professional or other personal interest of any nature or kind in any product, service and/or company that could be construed as influencing the

position presented in, or the review of, the manuscript entitled “Recovery of Copper, Lead, Zinc, and Arsenic from Copper Smelting Dust by Oxidative Alkaline Leaching and Sulfide Precipitation”.

REFERENCES

1. P.I. Grudinsky, V.G. Dyubanov, and P.A. Kozlov, *Russ. Metall. Met.* 2018, 7 (2018).
2. L. Guo, J. Lan, Y. Du, T.C. Zhang, and D. Du, *J. Hazard. Mater.* 386, 121964 (2020).
3. Z. Guo, D. Zhu, J. Pan, W. Yao, W. Xu, and J. Chen, *JOM* 69, 1688 (2017).
4. J. Che, W. Zhang, B. Ma, Y. Chen, L. Wang, and C. Wang, *Sci. Total Environ.* 843, 157063 (2022).
5. Y. Chen, S. Zhu, P. Taskinen, N. Peng, B. Peng, A. Jokilaakso, H. Liu, Y. Liang, Z. Zhao, and Z. Wang, *Miner. Eng.* 164, 106796 (2021).
6. X. Guo, L. Zhang, Q. Tian, D. Yu, J. Shi, and Y. Yi, *Trans. Nonferr. Met. Soc. China* 29, 2213 (2019).
7. X. Min, Y. Liao, L. Chai, Z. Yang, S. Xiong, L. Liu, and Q. Li, *Trans. Nonferr. Met. Soc. China* 25, 1298 (2015).
8. T. Yang, X. Fu, W. Liu, L. Chen, and D. Zhang, *JOM* 69, 1982 (2017).
9. Y. Zhang, B. Jin, Y. Huang, Q. Song, and C. Wang, *Sep. Purif. Technol.* 220, 250 (2019).
10. Y. Chen, N. Liu, L. Ye, S. Xiong, and S. Yang, *J. Clean. Prod.* 176, 26 (2018).
11. W. Gao, B. Xu, J. Yang, Y. Yang, Q. Li, B. Zhang, G. Liu, Y. Ma, and T. Jiang, *Chem. Eng. J.* 424, 130411 (2021).
12. A.S. Jones, J. Marini, H.M. Solo-Gabriele, N.M. Robey, and T.G. Townsend, *Waste Manag.* 87, 731 (2019).
13. R. Maal-Bared, R. Li, and A. Suarez, *Waste Manag.* 138, 19 (2022).
14. W. Zhang, J. Che, P. Wen, L. Xia, B. Ma, J. Chen, and C. Wang, *J. Hazard. Mater.* 416, 126149 (2021).
15. B. Xu, Y. Ma, W. Gao, J. Yang, Y. Yang, Q. Li, and T. Jiang, *JOM* 72, 3860 (2020).
16. X. Li, D. Liu, J. Wang, and J. Song, *Sep. Sci. Technol.* 55, 88 (2020).
17. Z. Pu, J. Han, Y. Li, Y. Dai, B. Yang, and A. Wang, *Mater. Trans.* 59, 311 (2018).
18. W. Zhang, J. Che, L. Xia, P. Wen, J. Chen, B. Ma, and C. Wang, *J. Hazard. Mater.* 412, 125232 (2021).
19. Y. Zhang, X. Feng, L. Qian, J. Luan, and B. Jin, *J. Environ. Chem. Eng.* 9, 105997 (2021).
20. G. Zheng, J. Xia, H. Liu, and Z. Chen, *J. Clean. Prod.* 283, 125384 (2021).
21. J. Xue, D. Long, H. Zhong, S. Wang, and L. Liu, *J. Hazard. Mater.* 413, 125365 (2021).
22. W. Tongamp, Y. Takasaki, and A. Shibayama, *Hydrometallurgy* 101, 64 (2010).
23. D. Li, X. Guo, Z. Xu, Q. Tian, and Q. Feng, *Hydrometallurgy* 157, 9 (2015).
24. Y. Wang, X. Liu, J. Yan, and S. Ye, *Resour. Conserv. Recycl.* 167, 105388 (2021).
25. A.F.D. de Namor, N.A. Hakawati, W.A. Hamdan, R. Soualhi, S. Korfali, and L. Valiente, *J. Hazard. Mater.* 326, 61 (2017).
26. J. Lei, B. Peng, Y.-J. Liang, X.-B. Min, L.-Y. Chai, Y. Ke, and Y. You, *Hydrometallurgy* 177, 123 (2018).
27. A.M. Nazari, R. Radzinski, and A. Ghahreman, *Hydrometallurgy* 174, 258 (2017).
28. Z.Y. Zhang, F.S. Zhang, and T. Yao, *Waste Manag.* 68, 490 (2017).
29. F. Kukurugya, E. Kim, P. Nielsen, L. Horckmans, J. Spoonren, K. Broos, and M. Quaghebeur, *Hydrometallurgy* 171, 245 (2017).
30. G. Yu, Y. Zhang, S. Zheng, X. Zou, X. Wang, and Y. Zhang, *Trans. Nonferr. Met. Soc. China* 24, 1918 (2014).
31. K. Gu, W. Li, J. Han, W. Liu, W. Qin, and L. Cai, *Sep. Purif. Technol.* 209, 128 (2019).
32. X. Zhang, J. Tian, H. Han, W. Sun, Y. Hu, T.Y. Li Wang, Y. Yang, X. Cao, and H. Tang, *Sep. Purif. Technol.* 238, 116422 (2020).
33. X. Lv, G. Li, Y. Xin, K. Yan, and Y. Yi, *Min. Metall. Explor.* 38, 2133 (2021).
34. M. Şahin, and M. Erdem, *Hydrometallurgy* 153, 170 (2015).
35. L. Tian, L. Huang, J. Xu, X. Yu, and Z. Xu, *Hydrometallurgy* 199, 105528 (2021).
36. H. Nie, C. Cao, Z. Xu, and L. Tian, *Sep. Purif. Technol.* 231, 115919 (2020).

Publisher's Note Springer Nature remains neutral with regard to jurisdictional claims in published maps and institutional affiliations.

Springer Nature or its licensor (e.g. a society or other partner) holds exclusive rights to this article under a publishing agreement with the author(s) or other rightsholder(s); author self-archiving of the accepted manuscript version of this article is solely governed by the terms of such publishing agreement and applicable law.